

A New Strictly Alternating Comblike Amphiphilic Polymer Based on PEG. 2. Associative Behavior of a High Molecular Weight Sample and Interaction with SDS

C. Heitz,[†] R. K. Prud'homme,[‡] and J. Kohn^{*,†}

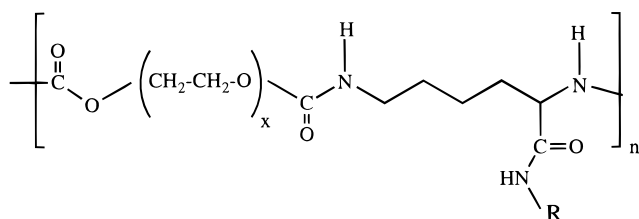
Department of Chemistry, Rutgers—The State University of New Jersey, Piscataway, New Jersey 08854, and Department of Chemical Engineering, Princeton University, Princeton, New Jersey 08544

Received July 16, 1999

ABSTRACT: We describe the associative behavior of a strictly alternating comblike amphiphilic polymer in aqueous surfactant (sodium dodecyl sulfate (SDS)) solutions. The polymer contains normal stearyl pendent hydrophobic groups separated by poly(ethylene glycol) (PEG) of molecular weight 8000. The average number of hydrophobes per chain is 9. In the dilute regime in the presence of very low amount of SDS, the polymer associates mainly in flowerlike micelles very similar to those formed by a sample of similar structure but a lower degree of polymerization (on average, two to three hydrophobes per chain). Further addition of SDS leads to the formation of mixed micelles of decreasing N_R (number of hydrophobes from the polymer per micelle). Flowerlike conformation is preserved until a SDS concentration which coincides with the critical aggregation concentration (cac) of SDS in the presence of poly(ethylene oxide) (PEO), after which the structure is disrupted. In the absence of SDS, below the polymer overlapping concentration c^* , bridging between micelles leads to phase separation between a highly viscous phase rich in polymer (network of interconnected flowerlike micelles) and a phase of very low viscosity. In the semidilute regime, the viscosity against SDS concentration exhibits a maximum, a classical result for hydrophobically modified polymers interacting with surfactant micelles. The covalent linkage between the PEG–C18 sequences belonging to the same polymer chain that bridges multiple micelles is responsible for the enhanced viscosity as compared to the telechelic PEO. Rheological data show evidence of the transition from a network of interconnected flowerlike micelles to an extended uniformly connected network upon addition of SDS.

Introduction

In the preceding paper, we described the synthesis of a strictly alternating amphiphilic polymer containing hydrophobic $C_{18}H_{37}$ groups separated by poly(ethylene glycol) (PEG) blocks of low polydispersity.¹ The polymer has the following structure:



Three samples of different degree of polymerization were synthesized and their molecular weight distribution was determined by gel permeation chromatography (GPC):

S28: $M_w = 28\,000$; $M_n = 18\,000$

S68: $M_w = 68\,000$; $M_n = 42\,000$

S113: $M_w = 113\,000$; $M_n = 74\,000$

* To whom correspondence should be addressed. Rutgers—The State University of New Jersey, Wright-Rieman Laboratories, Chemistry, 610 Taylor Rd., Piscataway, NJ 08854-8087. Telephone: (732) 445-3888. Fax: (732) 445-5006. E-mail: Kohn@rutchem.rutgers.edu.

[†] Rutgers—The State University of New Jersey.

[‡] Princeton University.

The associative behavior in water of the sample of lower molecular weight, S28, which contains on average two to three hydrophobes per chain, has been described in the companion paper. At low concentrations, S28 associates mainly in the form of individual flowerlike micelles resembling those formed by telechelic associative polymers. The same type of structure was also shown recently for random comblike polymers with $C_{14}H_{29}$ hydrophobes and PEG 8400 spacer blocks.² Micelles of S28 have a size of approximately 18 nm and contain on average four to five chains and a total of approximately 14 hydrophobic units. Association begins at concentrations lower than 0.02%. At a concentration higher than 2%, the system exhibits a large increase in viscosity, indicating the formation of larger aggregates. In this paper, we wish to study the association of the sample of higher molecular weight, S113, which contains on average 13 (calculated from M_w) or 9 (calculated from M_n) hydrophobic units per chain. In dilute aqueous solution, this polymer exhibits a phase separation between a gellike phase and a liquid phase. Phase separation is prevented in the presence of very low amount of a low molecular weight surfactant, sodium dodecyl sulfate (SDS). Therefore, in the dilute regime, characterization of the associative behavior is done in the presence of a very low amount of SDS, close to the minimum required to avoid phase separation, using static and dynamic fluorescence, dynamic light scattering, and viscosity measurement. The rheological behavior is examined in the absence of SDS in a more concentrated solution. In the second part of this paper, we examine the interaction with SDS and the evolution of the polymer structure upon addition of SDS.

Materials and Methods

Materials. Pyrene (99% pure), dimethylbenzophenone (DMBP) (99% pure) and sodium dodecyl sulfate (SDS) (99% pure) were obtained from Aldrich. Hexadecylpyridinium chloride (HDPC) (98% pure) was obtained from Fluka. Poly(ethylene oxide) (PEO) 93 500 (standard) was obtained from Polymer Laboratories.

Methods. Dynamic Light Scattering (DLS). The polarized DLS measurements in the homodyne mode were performed using the experimental setup described elsewhere.¹ The intensity autocorrelation function $g_2(t)$ was measured at 90°. The temperature was set at 25 °C. The solutions were prepared in Milli-Q water and filtered through 0.2 μm Acrodisc filters directly into the scattering cells. The intensity autocorrelation function $g_2(t)$ is related to the electric field autocorrelation function $g_1(t)$ through the Siegert relation

$$g_2(t) = 1 + b g_1(t)^2 \quad (1)$$

where b is an instrumental parameter.

The data were analyzed using the Brookhaven CONTIN version 5.0 software.

Rheology. The steady shear viscosities were measured at 25 °C using three different devices: a capillary viscometer (Ubbelohde, capillary diameter: 0.57 mm); a low shear rotational viscometer (Contraves LS30 used at shear rates from 0.5 to 100 s^{-1} with a Couette geometry); a rotational rheometer (Rheometrics RFS2 rheometer with a 50 mm parallel plate geometry). The latter device was also used for measuring the oscillatory shear response.

The reduced viscosity, η_{red} , of the polymer was calculated from the formula

$$\eta_{\text{red}} = (\eta - \eta_0)/\eta_0 c \quad (2)$$

where η_0 is the viscosity of the solvent, η the viscosity of the solution, and c the concentration in polymer, expressed in g/mL.

Spectrofluorimetry.³ The ratio I_1/I_3 of the intensity of the first and third emission peaks in the fluorescence emission spectra of pyrene was determined as described elsewhere.¹

Time-Resolved Fluorescence Quenching (TRFQ). A Photochemical Research Associates (PRA) model 3000 Fluorescence Lifetime Instrument (FLI) was used to determine the concentration of micelles in the polymer-surfactant mixtures by the time-resolved fluorescence quenching method,^{3,4} with pyrene as the probe. Quenchers were dimethylbenzophenone (DMBP) at high polymer concentration ($c_p = 2\%$), and hexadecylpyridinium chloride (HDPC) at low polymer concentration (0.3%). The concentration in micelles is determined from the adjustment of the fluorescence decay curves to the Infelta equation:

$$I(t) = I(0) \exp(-A_2 t - A_3 [1 - \exp(-A_4 t)]) \quad (3)$$

In the case where the distributions of probe and quencher over the micelles are frozen on the fluorescence time scale, the expressions for A_2 , A_3 and A_4 are

$$A_2 = k_0; \quad A_4 = k_Q; \quad A_3 = [Q]_m/[M] \quad (4)$$

where $k_0 = 1/t_0$ is the fluorescence decay rate constant of the probe in the micelles without quencher, $[Q]_m$ and $[M]$ are the concentrations of quencher in the micelles and of the micelles, respectively, and k_Q is the rate constant for intramolecular quenching. The concentration of pyrene was kept below 5% of the concentration of micelles $[M]$ to prevent excimer formation and the concentration of quencher $[Q]$ was adjusted such that $[Q]/[M]$ was around 1. The measurements were made on aerated samples.

Results and Discussion

Characterization of the Structures Formed in Pure Water or in the Presence of a Low Amount

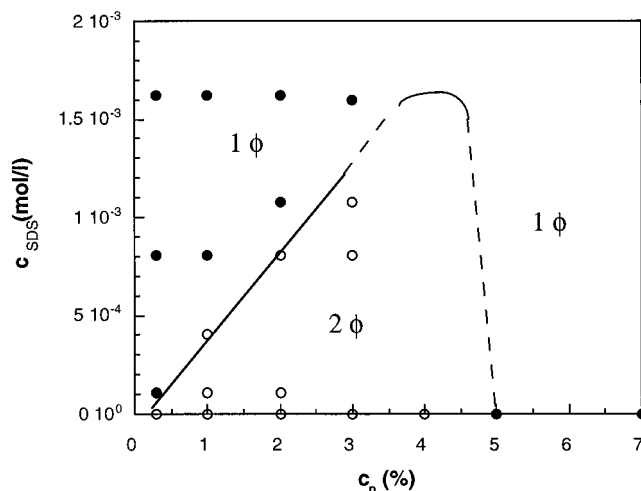


Figure 1. Phase diagram of S113 as a function of polymer concentration and SDS concentration: 1 phase (●); 2 phases (○).

of SDS. Phase Diagram. In deionized water in the absence of SDS, the phase diagram for S113 was studied at room temperature in the polymer concentration range 0.1 to 10%, as shown in Figure 1. The polymer was stirred in water for 24 h, and the solutions were then observed visually. Up to a concentration of 5%, the polymer phase separates into a gel like (slightly turbid) phase at the bottom and a liquid-phase poor in polymer at the top. The ratio between the volumes of the gel and solution phase increased with concentration. At concentration higher than 5%, the gel phase filled the entire volume. This behavior is different from the lower molecular weight sample ($M_w = 28\,000$), which did not phase separate. For S68 ($M_w = 68\,000$), phase separation was also observed, but in this case the gel phase was considerably reduced in volume as compared to S113 and the major part of the polymer was contained in the supernatant phase. Recently, fully end-capped telechelic polymers have been shown to phase separate upon dilution.⁵⁻⁷ The concentration of 5% at which the gel phase occupies all the volume for S113 coincides with the overlapping concentration c^* of the flowerlike micelles determined from the intrinsic viscosity of S28 in water.

For S113 at $c_p = 1\%$, we isolated the polymer contained in the upper solution phase by freeze-drying. Its molecular weight was measured by GPC in DMF and was found to be lower ($M_w = 77\,000$) than the molecular weight of the original polymer ($M_w = 113\,000$). Hence, the phase separation acts as a fractionation, the highest molecular weight chains being concentrated in the gel phase.

Addition of a small amount of SDS was shown to prevent phase separation (Figure 1). We determined the minimum concentration of SDS, c_{SDS} , needed to eliminate phase separation at various polymer concentrations. At $c_p = 0.3\%$, c_{SDS} was around 1×10^{-4} M. This is well below the critical micellar concentration (cmc) of SDS in pure water (8.1×10^{-3} M) and corresponds to 0.3 molecule of SDS per 1 stearylamine unit. The value of c_{SDS} increases almost proportionally with c_p .

Dilute Regime ($c_p = 0.3\%$): Fluorescence, Dynamic Light Scattering and Viscosity. To prevent phase separation, it was necessary to add a small amount of SDS in order to study the polymer association. The ratio of the total concentration of SDS in

Table 1. Fluorescence Lifetime t , Parameters Obtained from Equations 3 and 4 by Fitting Equation 3 to the Experimental Data and Aggregation Number N_R (of Polymer Hydrophobes) at Different SDS Concentrations for S113 at $c_p = 0.3\%$

c_{SDS} (mM)	t (ns)	A_3	$k_Q \times 10^{-7}$ (s $^{-1}$)	A_2^{-1} (ns)	N_R	$[Q] \times 10^{-5}$ (M)	no. of SDS molecules per micelle ^a
0.54	229	1.1	1.25	229	11.9	3.31	17.9
1.00		1.01	1.56	221	10.9	3.28	30.1
2.75	217	0.795	1.73	221	7.6	3.70	
	217	0.953	1.94	215	6.9	4.89	53.5
3.92		0.848	2.28	211	5.3	5.55	
		0.914	2.42	206	4.9	6.40	56.0
4.74	206	1.01	2.83	204	3.7	9.63	49.7
6.39	208	0.928	2.81	215	2.8	11.93	49.7
7.97		0.885	3.02	206	2.1	15.00	46.9

^a Total number of SDS molecule in solution for one micelle. The number of SDS molecules in a micelle is not known.

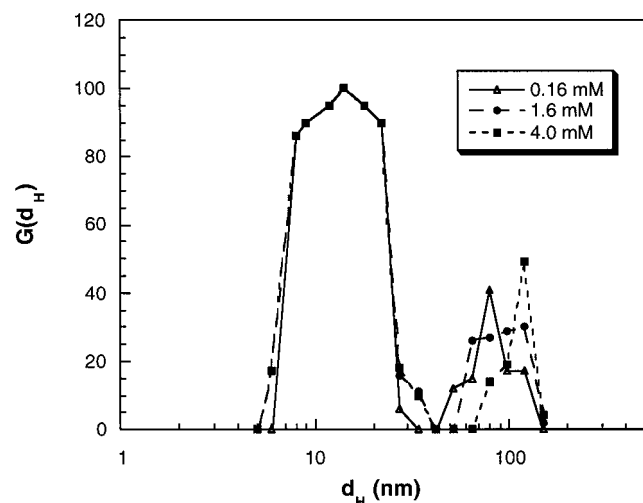


Figure 2. CONTIN distribution of the hydrodynamic diameters at $c_p = 0.3\%$. Concentration of SDS: 0.16 mM (Δ); 1.6 mM (\bullet); 4.0 mM (\blacksquare).

solution to the concentration of hydrophobes from the polymer was kept below or close to one.

Hydrophobic Association. The decay of the pyrene fluorescence in S113 solution in the presence of 0.54 mM SDS was monoexponential. The fluorescence lifetime, shown in Table 1, was 229 ns, well above the value for pyrene in water, which is around 120 ns in nondegassed solution. This establishes that pyrene is entirely solubilized in an hydrophobic environment, and also that there is only one type of hydrophobic host for the pyrene. I_1/I_3 values between 1.38 and 1.40 were measured in the SDS concentration range between 0.16 and 2 mM. Those values are similar to the high concentration plateau value (1.40) measured for S28 in water,¹ suggesting that the hydrophobic domains formed by S113 and S28 have features in common.

Size of the Aggregates. Dynamic light scattering was performed in the presence of 0.16 mM SDS. The distribution of sizes in Figure 2 exhibits two peaks. The maximum of the first peak (fast mode) corresponds to a diameter d_{Hf} of 14 nm, and the one of the second peak (slow mode) to a diameter d_{Hs} of 80 nm. Although the relative amplitude of the slow mode compared to the fast mode is not negligible (0.4), the weight concentration of the structure responsible for the slow mode will be small: At first approximation, the ratio of the weight concentration is given by the relative amplitude divided

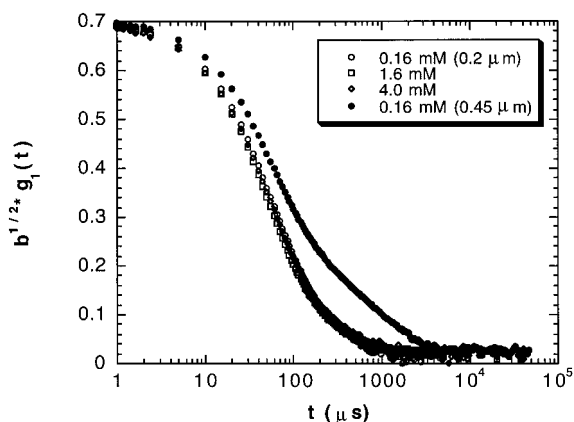


Figure 3. Time correlation functions $g_1(t)$ vs delay time measured at $\theta = 90^\circ$ at $c_p = 0.3\%$. Concentration in SDS: 0.16 mM (\circ); 1.6 mM (\square); 4.0 mM (\diamond); 0.16 mM filtered through 0.45 μ m pore filter (\bullet).

by the relative molar masses M_s/M_f , which is equal to $(d_{Hs}/d_{Hf})^3$ if we assume constant density. This gives a ratio of weight concentration of 0.002. However, there is evidence that filtration removed a certain amount of aggregates of larger size, as confirmed by the fact that the decay of the autocorrelation function is much slower after filtration through a larger pore size filter (0.45 μ m) (Figure 3). The slow mode will not be discussed here. The diameter at the maximum of the peak corresponding to the fast mode is rather close to the size of the flowerlike micelles formed by S28, a polymer of similar structure but lower degree of polymerization (between 16 and 20 nm).¹ It should be noted, however, that the hydrodynamic diameter of a PEO sample of molecular weight 113 000 calculated using the Devanand and Selser relationship for PEO in water at 30 $^\circ$ C⁸ is 22 nm from eq 5, which is not too different than the sizes corresponding to the fast mode.

$$R_H = 0.145 M_w^{0.571} (\text{\AA}) \quad (5)$$

Viscosity. The reduced viscosity at $c_{SDS} = 0.16$ mM is 42 mL/g, as compared to 122 mL/g for PEO homopolymer of similar molecular weight. The comb polymer adopts a much more compact structure than the homopolymer. This excludes the possibility that the species responsible for the fast mode and corresponding to size of the order of 14 nm could be unassociated, free polymer chains.

Discussion of the Results Obtained at 0.3%. It is evident that S113 associates, at least intramolecularly, via hydrophobic interactions at this concentration. If no association were to occur, the local concentration of hydrophobes in the volume occupied by one chain of S113 (evaluated from eq 5) would be 0.0027 M. This is 30 times higher than the upper concentration of the micellization region for a telechelic PEO of molecular weight 20 000 with C18 alkyl ends.⁶ The concentration of SDS used for the fluorescence experiment (0.54 mM) was much lower than the cmc of SDS in pure water (around 8 mM) and the cac (critical aggregation concentration) of SDS in the presence of PEO (around 4 mM). Thus, hydrophobic microdomains that solubilize pyrene result from the association of the hydrophobes from the polymer, although SDS probably binds to some extent to the existing polymer micelles. The low value of the reduced viscosity and the DLS results indicate that intermolecular association forming loose, extended

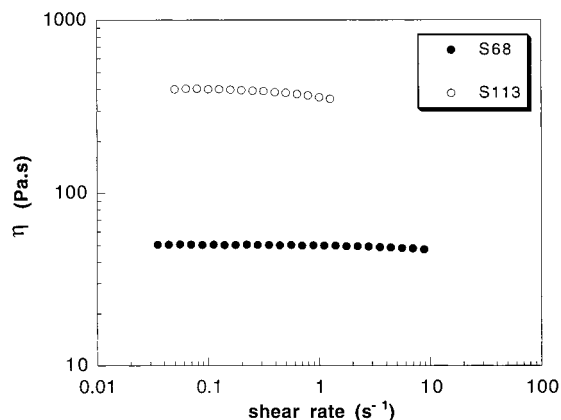


Figure 4. Viscosity vs shear rate: S68 (●); S113 (○).

aggregates does not occur to a great extent. Compact objects, resulting essentially from intramolecular association are formed predominantly. Since the average number of hydrophobes per chain is rather low (13 from M_w and 9 from M_n), formation of more than one micelle by one polymer chain is also precluded. The results support the formation of isolated flowerlike micelles from the association of the hydrophobes of one or more entire polymer chains. The flowerlike micelles are very similar to the ones formed by S28 in pure water, since both their size and the I_1/I_3 are close to the one formed by S28. The flower geometry is governed by the hydrophobe size and the entropy/excluded volume interactions of the solvated loops, but not by the connectivity of loops. The slow mode observed by DLS has not been discussed so far. We suggest that the structures responsible for this mode can be bridged flowerlike micelles. Obviously, given the polydispersity of the sample, some chains contain a number of hydrophobes much higher than the average N_R and could then participate in more than one micelles, connected together. Micelles containing a noninteger number of polymer chains will also be involved in bridge.

The aggregation number of the flowerlike micelles in the presence of a small amount of SDS (0.54 mM) was estimated by TRFQ. HDPC was used as the quencher. The parameters used to calculate the concentration of micelles from eq 4 were obtained by fitting eq 3 to the experimental data, assuming $[Q]_m = [Q]$. This assumption will be discussed later, along with other requirements that need to be fulfilled in order to use eqs 3 and 4. The aggregation number N_R was derived by assuming that all the stearyl amides are in the micelles. This gives $N_R = 12$. As discussed in more detail later, this value may be an underestimation of the aggregation number. However, $N_R = 12$ is close to the value obtained by light scattering for the flowerlike micelles formed by S28 (between 12 and 14).

Semidilute Regime: Rheology and Phase Behavior. Rheology. In deionized water, the steady shear and linear viscoelastic measurements were carried out at $c_p = 6\%$. This is slightly higher than the minimum concentration at which the solution becomes monophasic (5%), and corresponds to a weakly compressed gel. Measurements were made on both the S68 and the S113 samples.

Figure 4 gives the steady shear viscosity vs shear rate for the two polymers. The viscosity is Newtonian over the range of shear rates studied for S68. A slight shear thinning effect is noticeable for S113 for shear rates

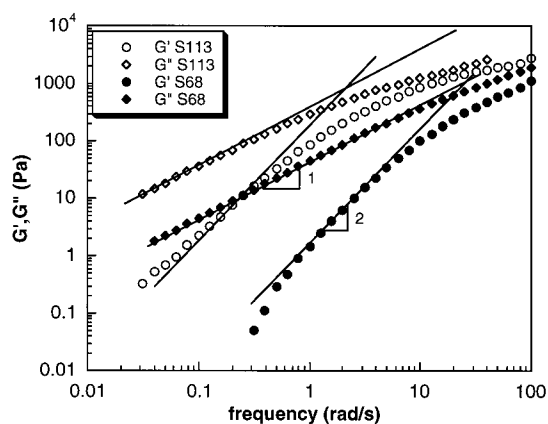


Figure 5. Storage modulus G' and loss modulus G'' vs frequency at $c_p = 6\%$: S68 (●, ◆); S113 (○, ◇).

higher than 0.1 s^{-1} . The zero shear viscosity is about 8 times higher for S113 ($\eta = 400 \text{ Pa}\cdot\text{s}$) than for S68 ($\eta = 50 \text{ Pa}\cdot\text{s}$).

The measured values of G' (storage modulus) and G'' (loss modulus) vs frequency ω for S68 and S113 are plotted in Figure 5. No plateau of G' was observed at high frequency. G' and G'' did not show simple Maxwellian behavior characterized by a single relaxation time; the samples exhibited a distribution of relaxation times. The same observation for solutions of random comblike associative polymers was made by Xu et al.⁹ This behavior is different from the telechelic polymers, which are characterized by a single relaxation time, attributed to the exit rate of the hydrophobe group from a micelle.¹⁰ In the case of our comblike polymers, because of the chemical linkage between hydrophobes belonging to the same polymer chain, the disengagement of one hydrophobe from one micelle will not lead to complete relaxation of the stress on the polymer chain; the chain is still linked to the micellar junction through other hydrophobes.

The longest relaxation times for the solutions are reflected in the terminal behavior at low frequencies where $G' \sim \omega^2$ and $G'' \sim \omega^1$.¹¹ Lines with slopes of 1 and 2 are drawn through the data in Figure 5. As is normally found, the slope of 1 in the terminal regime is obtained precisely for the loss modulus G'' . There is some curvature of the data for the storage modulus G' , which is caused by a lack of instrument resolution at the lowest frequencies since the fraction of the stress in G' is less than 1% of the stress in G'' . The intersection point of the extrapolated lines for G' and G'' gives the high-frequency plateau modulus G_∞ and the relaxation time τ of the contribution of the longest relaxation process. They are

$$\text{for S113: } G_\infty = 840 (\pm 200) \text{ Pa} \quad \tau = 0.45 \text{ s}$$

$$\text{for S68: } G_\infty = 1100 (\pm 200) \text{ Pa} \quad \tau = 0.038 \text{ s}$$

The zero shear viscosity calculated from the relation $\eta = G_\infty \tau$ gives $\eta = 380 \text{ Pa}\cdot\text{s}$ for S113 and $\eta = 42 \text{ Pa}\cdot\text{s}$ for S68, in good agreement with the measured values of 400 and 50 $\text{Pa}\cdot\text{s}$, respectively.

The striking point is that G_∞ is almost identical for the two polymers, whereas the viscosities (and the relaxation times) vary over 1 order of magnitude. It would have been interesting to measure G_∞ for S28 too, to confirm the invariance of G_∞ with the polymer molecular weight. Unfortunately, at this concentration,

the elastic modulus G' falls below the resolution of the rheometer over the range of accessible frequencies.

The theory of Semenov et al.¹² established for flower-like micelles of telechelic polymers predicts that the elastic modulus of the weakly compressed micellar gel (i.e., at concentration only slightly higher than the concentration of the uncompressed micellar gel) is dominated by the osmotic compressibility of the gel. The contribution of the bridges to the elastic modulus is negligible. On the other hand, the theory of transient networks¹³ predicts that the elastic modulus varies as νkT , where ν is the number density of elastically active chains. The increase of comb polymer molecular weight increases the connectivity, but will not change the osmotic compressibility of the gel, which depends on the flower characteristics only. Our results show that this system behaves accordingly to Semenov's model in this concentration regime.

Phase Behavior. For polymer concentrations lower than 5%, we observed phase separation into a concentrated gel phase and an aqueous phase essentially free of polymer for sample S113 (Figure 1), while for the low molecular weight sample S28 no phase separation was observed over the same polymer concentration range. There are two possible explanations for this behavior: one having to do with the number of polymer chain that can be accommodated in a single flower micelle with the other explanation due to end effects for these looped polymers.

Semenov's model predicts a phase separation between a macrophase of close-packed micelles and a very dilute solution of micelles. According to Semenov et al., the energy of interaction between two flowers of telechelic polymers contains an attractive term due to bridging and an osmotic repulsive term. When the distance between flowers is such that the attractive term due to bridging dominates, there is phase separation. In our case, the molecular weight of the polymer seems to be the relevant parameter that regulates phase separation, and this suggests an additional mechanism. It seems that the bridging between micelles is only favored when the length of the polymer chain is such that one micelle cannot accommodate an integer number of polymer chains. This is obviously the case when the number of repeat units per polymer chain is larger than the aggregation number of one micelle, but also when it is slightly smaller. The formation of one micelle would then involve the contribution of part of a second polymer chain, whose remaining part belongs to another micelle, and then acts as a bridge. There is an other explanation to the observed difference of phase behavior as a function of the comb polymer molecular weight. Whereas phase separation was recently shown for fully end-capped telechelic PEO,⁵⁻⁷ incompletely functionalized samples do not phase separate, presumably because the free chain ends extending into the solution provide a steric barrier which prevents bridging association.⁶ Phase separation was not observed either for the random comblike polymers studied by Xu et al., and the authors also suggested that this could be due to the free chain ends.⁹ For the comb polymers studied here, the weight concentration of chain ends and in turn of PEG terminated chain ends increase when the degree of polymerization decrease, and those ends may provide a steric barrier which prevents bridging between micelles for the low molecular weight sample (S28).

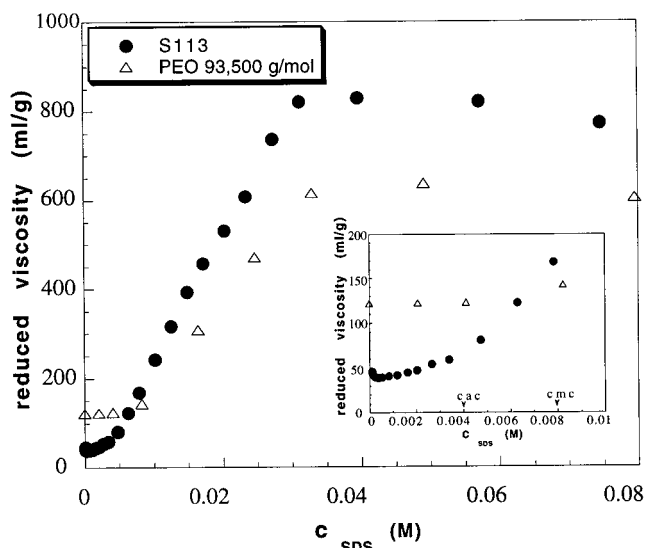


Figure 6. Reduced viscosity vs SDS concentration at $c_p = 0.3\%$: S113 (●); PEO 93 500 (△). In the inset window, the low SDS concentration portion of the curve is expanded. The arrows designate the position of the cmc of SDS in pure water and of the cac of SDS in the presence of PEO.

Polymer–Surfactant. Dilute Regime: $c_p = 0.3\%$. The interaction of SDS with PEO has been extensively studied in the literature using a variety of methods including surface tension,^{14,15} conductivity,^{14,16} gel filtration,¹⁷ viscosity,^{16,18} NMR,¹⁹ and neutron scattering.²⁰ The general scheme is that the interaction begins at an SDS concentration referred to as the critical aggregation concentration (cac) almost independent of the polymer concentration and equal to around 4×10^{-3} M.¹⁴⁻¹⁶ Above the cac, the surfactant binds to the polymer in the form of micellar aggregates until the polymer becomes saturated with surfactant, which occurs at an SDS concentration which depends on the polymer concentration.

Viscosity. The variation of the reduced viscosity η_{red} of the PEO 93 500 homopolymer against SDS concentration is shown in Figure 6. η_{red} increases from an SDS concentration of around 8×10^{-3} M and reaches a plateau at a concentration of 0.032 M. η_{red} increases due to the binding of micelles of SDS to the polymer, which leads to a charging of the polymer backbone.¹⁶ The plateau is reached at the saturation, and leads to a binding ratio of 0.38 SDS/EO, which is in good agreement with the literature values.

For the comb polymer S113, at the first stage of SDS addition, η_{red} is much lower than that of the homopolymer. After a slight decrease, η_{red} increases from $c_{SDS} = 0.54$ mM to approximately 4 mM and then increases more sharply from this value, which, interestingly, coincides with the cac of SDS with PEO. η_{red} reaches the same level as the homopolymer for SDS concentrations between 6 and 8 mM. From this point, the reduced viscosity of the two polymers behaves similarly. The reduced viscosity of the comb polymer is systematically slightly higher, which may be ascribed to the slight difference in molecular weight between the two polymers.

The low value of η_{red} at very low SDS concentration has been discussed above and is due to the compact flowerlike conformation of the comb polymer. At SDS concentrations above 6–8 mM (17 to 22 SDS per hydrophobe), the similarity of the viscosity behavior

indicates that the comb polymer adopts the same conformation as the homopolymer. In particular, the compact flowerlike structure may have been completely disrupted. Before this, two different regions of SDS concentration are distinguishable: $0 < c_{\text{SDS}} < c_{\text{ac}}$ and $c_{\text{ac}} < c_{\text{SDS}} < 6\text{--}8\text{ mM}$, where c_{ac} is defined as the c_{ac} of SDS in the presence of PEO. In the first region, interaction is expected to be driven essentially by hydrophobic interaction between SDS and the hydrophobes of the polymer. In the second region, SDS may interact with the PEO backbone, too. The sharp increase of viscosity at c_{SDS} above 4 mM suggests that the polymer conformation undergoes a large change in this region, whereas it is much less affected in the first region, where the viscosity increase is much smaller.

Dynamic Light Scattering. DLS experiments were performed in the region $0 < c_{\text{SDS}} < c_{\text{ac}}$.

The electric field autocorrelation functions $g_1(t)$ (Figure 3) at $c_{\text{SDS}} = 1.62\text{ mM}$ and $c_{\text{SDS}} = 4\text{ mM}$, as well as the CONTIN distribution of hydrodynamic diameters (Figure 2), are strikingly similar to the one obtained at $c_{\text{SDS}} = 0.16\text{ mM}$ discussed above. The distributions exhibit two peaks, the maximum of the fast mode is around 14 nm and the maximum of the slow mode around 100 nm. The relative amplitude of the slow to the fast mode was below 0.4 in all cases. However, as we discussed above, the structures responsible for the slow mode represent only a minute mass fraction. The fast mode was attributed to isolated flowerlike micelles at low SDS concentration (0.16 mM) (see above). The DLS results show that objects of similar conformation remain predominant within the whole $0 < c_{\text{SDS}} < c_{\text{ac}}$ region.

Aggregation Number. TRFQ experiments have been performed in the SDS concentration range in which the viscosity behavior differs from the homopolymer ($1.6 \times 10^{-4}\text{ M}$ to $8 \times 10^{-3}\text{ M}$). HDPC was used as the quencher. The parameters used to calculate the concentration in micelles from eq 4 were obtained by fitting eq 3 to the experimental data, which is appropriate providing the following conditions are verified. The probe and quencher must be immobile during the lifetime of the pyrene, their fraction in the micelles must be known, and the repartition of the quencher among the micelles must follow the Poisson distribution. Those points are discussed here. The decay of the fluorescence lifetime in the absence of quencher was monoexponential at all SDS concentrations investigated. The fluorescence lifetimes, shown in Table 1, fell between 229 and 206 ns, well above the value for pyrene in water (around 120 ns in nondegassed solution), establishing that pyrene is entirely solubilized in the micellar phase, and also that there is only one type of hydrophobic host for the pyrene. We assumed that all the quencher was in the micelles, i.e., $[Q]_{\text{m}} = [Q]$. Although the TRFQ experiments were conducted well below the cmc of the quencher in pure water (between $1/30$ and $1/7$ of the cmc; the cmc of HDPC is around 1 mM ²¹), a significant fraction of the quencher must be bound to the micelles. We showed that the interaction of SDS with S113 begins at an SDS concentration at least as low as the lowest concentration used for the TRFQ experiment (0.16 mM) and that S113 behaves as a polyamphiphile carrying negative charges coming from the bound SDS heads. Anthony et al. studied the interaction of a cationic surfactant (DTAC) with anionic polysoaps²² and showed that the fixation of the surfactant to the polymer was

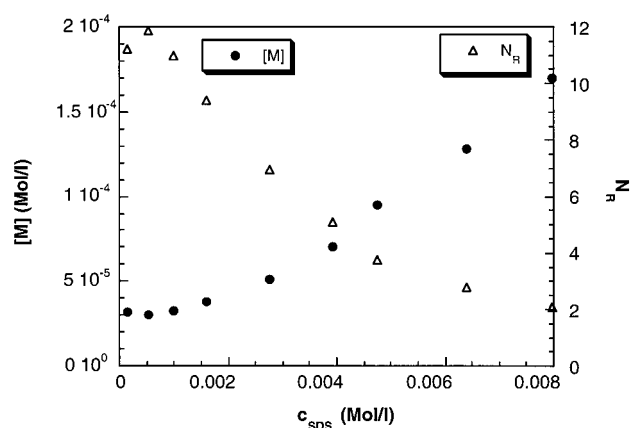


Figure 7. Concentration of micelle $[M]$ (●) and number of hydrophobes per micelle N_R (△) vs SDS concentration for S113 at $c_p = 0.3\%$.

almost complete at a concentration of surfactant several orders of magnitude lower than the cmc of the surfactant. If, however, some HDPC remains in the aqueous phase, assuming $[Q]_{\text{m}} = [Q]$ leads to an underestimation of N_R . Upon addition of SDS, both the increase of the hydrophobic volume and the further negative charging of the micelles due to fixation of more SDS increase the affinity of HDPC for the micelles, thereby reducing the proportion, if it is not zero, of quencher in the water phase. This decreases the possible error made on N_R . We observe (see below) a decrease of N_R with increasing c_{SDS} , so the trend of the variation of N_R upon addition of SDS remains meaningful, even if the absolute value of N_R is not exact. The fluorescence lifetimes t measured in the absence of quencher almost always coincide within 3% with A_2^{-1} , showing that exchange of quencher did not occur (Table 1). When the TRFQ experiment was performed at two quencher concentrations (for $c_{\text{SDS}} = 2.75$ and 3.72 mM), A_2^{-1} and k_q did not vary significantly, but the calculated aggregation number decreased slightly when $[Q]$ increased. This may indicate that the Poisson distribution is not fully satisfied, as also observed by Alami et al. in end capped PEO micelles.²³ They concluded that reliable values of N_R could not be obtained by the method in this case, mostly because the cmc of the polymer was not well located and because a broad distribution of micelles or aggregates of smaller size existed, all the way down to dimers. Aggregates involving such a small number of hydrophobes are not likely to form for the high molecular weight S113 sample. In our first paper we showed that S28 forms flowers of N_R much larger than the average number of hydrophobes per polymer (14 and 3, respectively). Furthermore, binding of SDS to the micellar core will not decrease its hydrophobic volume. For this reason, the system we study is probably closer to the Poisson distribution than was the system studied by Alami et al. However, small deviations are observed, maybe because the micelles are polydisperse. This issue was not addressed here. In all cases, the quencher concentration was chosen such that $[Q]/[M]$ was close to 1.

The addition of SDS leads to a continuous increase of $[M]$ (Figure 7). As shown in Table 1, we observed a decrease of the fluorescence lifetime t and an increase of the rate constant for fluorescence quenching, k_q , as the SDS concentration increases. The values of t at low SDS concentrations were much higher than in solutions of SDS above the cmc (170 ns at a SDS concentration of 0.14 M). The most probable reason for the high values

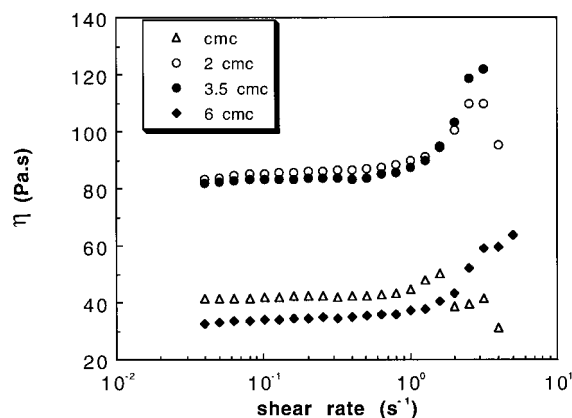


Figure 8. Viscosity vs shear rate at constant polymer (S113) concentration (2%) at different SDS concentrations: 8.1×10^{-3} M ($1 \times \text{cmc}$) (Δ); 1.62×10^{-2} M ($2 \times \text{cmc}$) (\bullet); 2.92×10^{-2} M ($3.6 \times \text{cmc}$) (\bullet); 4.86×10^{-2} M ($6 \times \text{cmc}$) (\blacklozenge).

of t is that the microviscosity of the micellar core is very high, making the quenching processes by dissolved oxygen less efficient.^{22,24,25} The same reason would explain the low k_Q values at low SDS concentration. In fact, micelles of HEUR polymers were shown to have very rigid cores and gave very low k_Q values.²⁶ The decrease of t and the increase of k_Q upon SDS addition may indicate an increase of the fluidity of the micelles, which may be due to the increase of the SDS/stearylamide ratio in the micelle. As shown in Figure 7, N_R dropped from 12 at low SDS concentration to around 2 at $c_{\text{SDS}} = 8 \times 10^{-3}$ M. The concentration in micelles increases already at $c_{\text{SDS}} < \text{cac}$, showing that SDS induces the formation of more micelles, and does not just "swell" the existing micelles. This may explain why low amount of SDS prevents phase separation. It is likely that SDS molecules replace stearylamine in the micelles while the number of micelles increases. For entropic reasons, the replacement will lead to the disengagement from the micelles of the polymer chains involved in links, resulting in a greater number of micelles containing an integer number of polymer chains. It is also possible that the micelles become repulsive because they are negatively charged by SDS, and this repulsion may overcome the bridging attraction. The increase of $[M]$, which is rather slow at the beginning of SDS addition, becomes stronger at a concentration around $0.35 \times \text{cmc}$ to $0.5 \times \text{cmc}$.

It is worth noting that both the reduced viscosity and the concentration of micelles increase more sharply beginning at the SDS concentration range which is close to the cac of SDS interacting with PEO. The DLS results strongly suggest that the flowerlike conformation is maintained until the cac. The viscosity results show that this structure is disrupted at 6–8 mM. This suggests that the transition from flowerlike micelles to "homopolymer" like conformation occurs between the cac and 6–8 mM. Below the cac, addition of SDS leads to the increase of the number of flowerlike micelles of decreasing aggregation number. The size of the flower like micelles is expected to decrease approximately as $N_R^{1/5}$ ²⁷ when N_R decreases. As N_R is approximately divided by 2 between $c_{\text{SDS}} = \text{cmc}/50$ and cac, the size of the flower is expected to decrease by a factor of 0.87. Such a small variation may not be noticeable by DLS.

Semidilute Regime: $c_p = 2\%$. Rheological Behavior. The viscosity against shear rate is given in Figure 8 for four different SDS concentrations. The

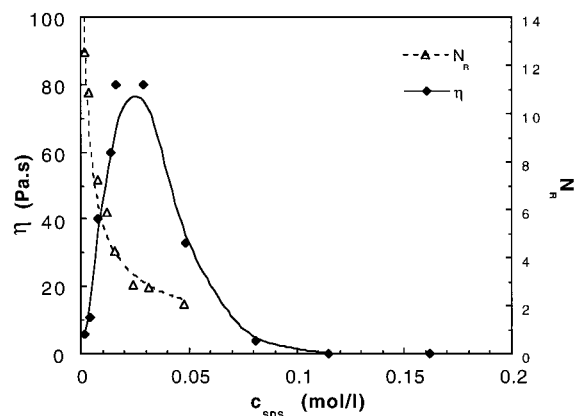


Figure 9. Zero shear viscosity η (\blacklozenge) and number of hydrophobes per micelle N_R (Δ) vs SDS concentration at constant polymer (S113) concentration (2%). The lines are guides for the eyes.

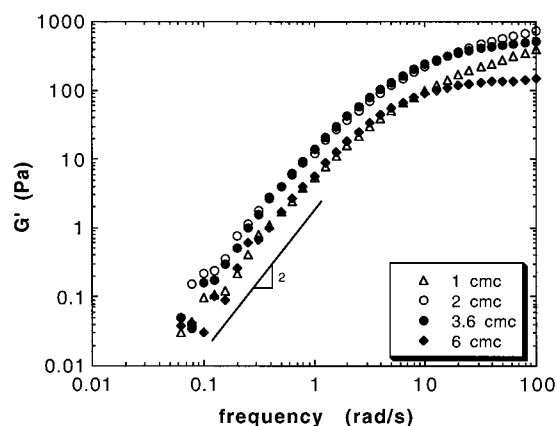


Figure 10. Storage modulus G' vs frequency at constant polymer (S113) concentration (2%) at different SDS concentrations: 8.1×10^{-3} M ($1 \times \text{cmc}$) (Δ); 1.62×10^{-2} M ($2 \times \text{cmc}$) (\circ); 2.92×10^{-2} M ($3.6 \times \text{cmc}$) (\bullet); 4.86×10^{-2} M ($6 \times \text{cmc}$) (\blacklozenge).

viscosity is Newtonian at low shear rate and exhibits shear thickening at high shear rate. The shear thickening effect increases with increasing SDS concentration.

The viscosity dependence on the concentration of SDS is illustrated in Figure 9. The viscosity exhibits a maximum, extending approximately from 0.016 to 0.032 M (2 to 4 times the cmc of SDS in pure water), which corresponds to 7 to 14 SDS molecules per hydrophobe. The complete disintegration of the network (very low viscosity) occurs at concentration equal to around 0.11 M (14 times the cmc), i.e., 48 SDS molecules per hydrophobe, which is a number close to the aggregation number of a pure SDS micelle.

The storage modulus G' and the loss modulus G'' vs frequency at 4 different SDS concentrations are given in Figures 10 and 11, respectively. G' and G'' vary as ω^2 and ω , respectively, in the low-frequency range for all the SDS concentrations. However, G' does not reach a plateau, and the plot of G' vs frequency exhibits a pronounced curvature. This shows that the solutions exhibit a distribution of relaxation times. The distribution of relaxation times narrows when the concentration in SDS increases, and at the highest concentration studied ($6 \times \text{cmc}$), it is close to a single relaxation time with G' approaching a plateau at high frequencies. This suggests that, at low SDS concentration, the solution retains a flowerlike conformation, with multiple relax-

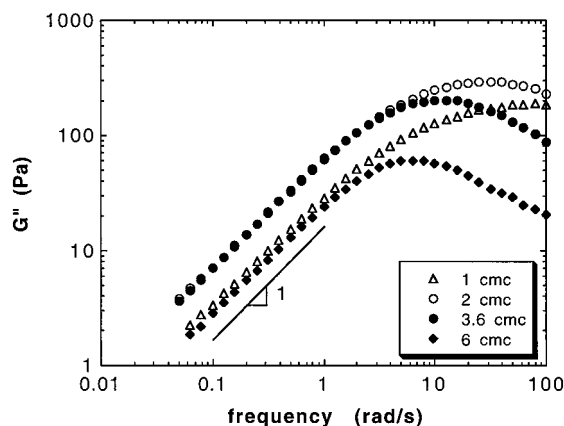


Figure 11. Loss modulus G'' vs frequency at constant polymer (S113) concentration (2%) at different SDS concentrations: 8.1×10^{-3} M ($1 \times \text{cmc}$) (Δ); 1.62×10^{-2} M ($2 \times \text{cmc}$) (\circ); 2.92×10^{-2} M ($3.6 \times \text{cmc}$) (\bullet); 4.86×10^{-2} M ($6 \times \text{cmc}$) (\blacklozenge).

Table 2. Fluorescence Lifetime t , Parameters Obtained from Equations 3 and 4 by Fitting Equation 3 to the Experimental Data and Aggregation Number N_R (of Polymer Hydrophobes) at Different SDS Concentrations for S113 at $c_p = 2\%$

c_{SDS} (mM)	t (ns)	A_3	$k_Q \times 10^{-7}$ (s $^{-1}$)	A_2^{-1} (ns)	N_R	$[Q] \times 10^{-5}$ (M)	no. of SDS molecules per micelle ^a
1.54	236	0.996	1.77	246	12.55	1.864	8.2
3.86		0.848	2.12	231	10.85	1.836	17.8
7.89		0.565	2.53	233	7.48	1.776	
		1.01	3.07	231	7.25	3.276	24.3
11.87		0.801	3.57	223	5.90	3.193	29.8
16.00		0.663	3.82	219	5.04	3.097	
		0.819	4.01	219	4.23	4.555	
		1.08	4.49	221	4.29	5.916	29.2
23.98		0.788	4.84	211	3.32	5.58	
		0.929	4.50	212	2.87	7.62	29.2
31.6		0.841	4.72	207	2.75	7.187	37.0
47.63		0.595	5.04	194	2.23	6.283	
		0.965	5.12	201	2.07	11.01	41.7

^a Total number of SDS molecule in solution for one micelle. The number of SDS molecules in a micelle is not known.

ation times. The addition of SDS progressively leads to the transition from connected flowers to a uniformly connected network where stress relaxation is governed by a random first-order process consistent with transient network theories.^{13,28} This would apply in the situation where the bridging between polymer chains is a micelle containing essentially SDS and only a few hydrophobes from different polymer chains. On the other hand, the connected flowers characterized by multiple relaxation times each contain many hydrophobes and the modulus is determined by excluded volume interactions between flowers.

Aggregation Number. TRFQ experiments were performed in the SDS concentration range where the rheology data showed a transition from a broad to narrow distribution of relaxation rates. DMBP was used as the quencher. At the lowest SDS concentration studied (1.54 mM), the fluorescence decay was obtained in the absence of quencher. The decay was monoexponential, and the fluorescence lifetime t (see Table 2) was much higher than that for pyrene dissolved in water. A_2^{-1} and t agreed within 4%, so exchange of the quencher does not occur. The decay in the absence of quencher was not recorded at higher SDS concentration. Using the same probe and quencher, van Stam et al.

studied by TRFQ the interaction between SDS and PEO at PEO concentration of 2%²⁹ and did not observe any effect due to quencher migration. The viscosity of the solutions renders the determination of the partition coefficient of DMBP between the micelles and the water phase impossible for our system at this polymer concentration. Van Stam et al. reported a value of K_D of 1900 M^{-1} for DMBP in 2% PEO and 20 mM SDS solution,³⁰ where

$$[Q]_m/[Q]_{aq} = K_D S_m \quad (6)$$

with $[Q]_m$ and $[Q]_{aq}$ the concentration of quencher in the micellar phase and in the water phase, respectively, and S_m the concentration of surfactant in the micelles. For our system, S_m can be expressed as $S_m = c_p(M) + [\text{SDS}]_m$, where $c_p(M)$ is the concentration of hydrophobes from the polymer and $[\text{SDS}]_m$ is the concentration of SDS in the micelles. $[\text{SDS}]_m$ is not known. At SDS concentration lower than the cac of SDS in the presence of PEO (around 4×10^{-3} M), S_m is at least equal to c_p , which gives $[Q]_m = 0.82[Q]$. Above the cac of SDS in the presence of PEO, $[\text{SDS}]_m$ is at least equal to $[\text{SDS}] - \text{cac}$, from which $[Q]_m$ is above $0.92[Q]$ at an SDS concentration above 8.1×10^{-3} M. We then assume $[Q]_m = [Q]$, which appears to us to be a valid approximation, at least at an SDS concentration above 8.1×10^{-3} M. As was the case at the lower polymer concentration studied before, the aggregation numbers derived by TRFQ were found to decrease slightly when $[Q]$ increases. This may also indicate that the Poisson distribution is not completely satisfied, and that use of eqs 3 and 4 for the determination of $[M]$ may be only approximate.

The variation of N_R upon the addition of SDS was derived by TRFQ, assuming that all the hydrophobes are in the micelles (we point out that there are no free SDS micelles in solution in the concentration range studied by fluorescence since we are below the saturation of polymer with SDS (around 3 EO per SDS, i.e., 0.15 M ($18 \times \text{cmc}$)). N_R (Figure 9) decreases from around 12 at the lowest concentration of SDS to around 2 for $c_{\text{SDS}} = 0.048 \text{ M}$ ($5.9 \times \text{cmc}$). In the range of concentration corresponding to the maximum of viscosity, N_R decreases from 4 (for $c_{\text{SDS}} = 2 \times \text{cmc}$) to 2.6 (for $c_{\text{SDS}} = 3.9 \times \text{cmc}$). We observed (Table 2) a decrease of A_2^{-1} and an increase of the rate constant for quenching, as was also the case for $c_p = 0.3\%$. This can be ascribed to the same reason: the increase of the fluidity of the micellar core resulting from the increase in the ratio of SDS to stearylamine. The fluorescence data support our interpretation of the rheological results: At $1 \times \text{cmc}$, where the rheological data show evidence of multiple relaxation times, the still relatively high value of N_R ($N_R = 7$) is consistent with the persistence of flowerlike micelles, whereas at $6 \times \text{cmc}$, where the rheological behavior is close to Maxwellian, N_R is equal to 2, indicating the disappearance of the flowers, but the retention of a still high viscosity.

It is interesting to compare our observations to those reported in the literature for hydrophobically end capped PEO interacting with SDS. A viscosity maximum is generally observed^{5,31–34} and has been interpreted as follows:³⁴ the addition of SDS increases the number of micelles in the system, which causes a transition from loops to bridges which will increase the viscosity. On the other hand, the addition of surfactant decreases the number of end groups per micelle, until

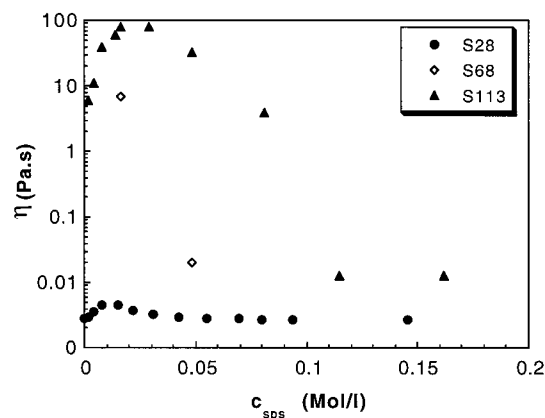


Figure 12. Zero shear viscosity η vs SDS concentration at constant polymer concentration (2%): S28 (●); S68 (◇); S113 (▲).

the network disintegrates when micelles containing one or two end groups are predominant.

For polymers of the HEUR type,⁵ $(\text{C}_{18}\text{H}_{37}\text{NHCOO})_2(\text{EO})_n$, with n between 182 and 663 and at a polymer concentration of 2%, the viscosity maximum was found to occur at an SDS/hydrophobe ratio comprised between 4 and 8, much lower than in the case of S113 for which the viscosity is still at its maximum level for a ratio of 14. In the particular case of $(\text{C}_{18}\text{H}_{37}\text{NHCOO})_2(\text{EO})_{182}$, for which the molecular weight of the PEO backbone is comparable to the PEG spacer of our sample, as is the hydrophobe length, the maximum of viscosity was around 2–3 Pa·s, much lower than the value of 80 Pa·s that we measured with S113. For end capped PEO, which contains two hydrophobes per chain, only the micellar junctions containing at least three hydrophobes can propagate the network, when two are sufficient for our sample, as the chains contain on average more than three hydrophobes. Indeed, for S113, the viscosity is still at its maximum level when N_R is equal to 2.6, a value for which the network would break down for a polymer bearing only two hydrophobes. This explains why the maximum is shifted to higher SDS/hydrophobe ratios in our case.

The importance of the chemical linkage between hydrophobes on the rheological behavior is highlighted in Figure 12, in which the zero shear viscosities vs SDS concentrations are compared for the three copolymers. It can be seen that the maximum is shifted to higher SDS/hydrophobe ratios and the viscosity value at the maximum increases when the molecular weight increases.

In the case of end-capped PEO, the viscosity at a given hydrophobe length is regulated by two opposing phenomena: interchain association is favored over intrachain association when the molecular weight increases, but at the same time, the hydrophobe content decreases. Hence, for the same hydrophobe, the viscosity vs molecular weight exhibits a maximum, both in pure water and in the presence of surfactant. In our case, by increasing the degree of polymerization, it is possible to increase the molecular weight without decreasing the hydrophobe content.

Conclusion

We have investigated the association in water of a strictly alternating comb copolymer with pendent $\text{C}_{18}\text{H}_{37}$ hydrophobic groups separated by PEG of molecular weight 8000. In dilute solution, the sample of highest

molecular weight (S113) exhibits a phase separation between a gel phase and a solution phase. The associative behavior was studied in the presence of low amount of SDS. The polymer associates mainly into isolated flowerlike micelles of size and aggregation number close to those formed by S28, a sample of the same structure but of lower degree of polymerization. However, a small fraction of the sample is involved in much larger aggregates which could result from bridging of flowers. Further addition of SDS leads to the formation of mixed micelles of decreasing N_R (number of hydrophobes from the polymer per micelle). Flowerlike conformation is preserved until a concentration in SDS which coincides with the cac of SDS in the presence of PEO, and is then disrupted. In the absence of SDS, above c^* , the elastic modulus of the slightly compressed gel does not vary with the molecular weight of the polymer but the relaxation time increases with increasing molecular weight. This is consistent with Semenov's model for flowerlike micelles in which the elastic modulus is dominated by the osmotic compressibility of the gel. In the semidilute regime, the viscosity vs SDS concentration exhibits a maximum. The value of the viscosity and the concentration of SDS at the maximum of viscosity both increase with the molecular weight of the polymer. With increasing SDS concentration, the dynamic viscoelastic behavior shows a transition from a network of interconnected flowers, characterized by a broad distribution of relaxation times, to an extended, uniformly connected network with a narrower spectrum of relaxation times. It should be noticed that the three polymers studied so far have an average number of hydrophobes per chain smaller than (or of the order of) the measured value of N_R . The case of polymer of much higher degree of polymerization, in which each chain could host several micelles would be of interest. In addition to the possibility of varying the overall molecular weight of the copolymer, the molecular architecture allows changes in the molecular weight of the PEG spacer and changes in the nature of the hydrophobic pendent chains independently of each other. This design provides a unique model system for the study of structure–property correlations which will prove valuable in testing newly evolving theories of comb copolymer structure and dynamics.

Acknowledgment. This work was supported by a seed grant from the New Jersey Center for Biomaterials and Medical Devices, by the New Jersey Commission on Science and Technology, and by NIH Grant GM39455. The authors thank the scientific staff of the Complex Fluids Laboratory at Rhodia, Inc., for stimulating discussions and for access to the light-scattering apparatus and the low shear viscosimeter. The authors also thank Professor G. Strauss for access to the fluorescence lifetime instrument and Mr. D. E. Weyand for access to the static fluorimeter.

References and Notes

- (1) Part 1. Heitz, C.; Prud'homme, R. K.; Pendharkar, S.; Kohn, J. *Macromolecules* **1999**, *32*, 6652.
- (2) Xu, B.; Li, L.; Zhang, K.; Macdonald, P. M.; Winnik, M. A. *Langmuir* **1997**, *13*, 6896–6902.
- (3) Zana, R. In *Surfactant Solutions*; Zana, R., Ed.; Marcel Dekker: New York and Basel, Switzerland, 1987; pp 241–294.
- (4) Infelta, P. *Chem. Phys. Lett.* **1979**, *61*, 88.
- (5) Kaczmariski, J. P.; Glass, J. E. *Macromolecules* **1993**, *26*, 5149–5156.

- (6) Maitre, S. Ph.D. Thesis, Université Louis Pasteur, Strasbourg, France, 1997.
- (7) Pham, Q. T.; Russel, W. B.; Lau, W. *J. Rheol.* **1998**, *42*, 159.
- (8) Devanand, K.; Selser, J. C. *Macromolecules* **1991**, *24*, 5943.
- (9) Xu, B.; Yekta, A.; Winnik, M. A.; Sadeghy-Dalivand, K.; James, D. F.; Jenkins, R.; Bassett, D. *Langmuir* **1997**, *13*, 6903–6911.
- (10) Annable, T.; Buscall, R.; Ettelaie, R.; Whittlestone, D. *J. Rheol.* **1993**, *37*, 695–726.
- (11) Ferry, J. D. *Viscoelastic Properties of Polymers*; Wiley: New York, 1980.
- (12) Semenov, A. N.; Joanny, J.-F.; Khokhlov, A. R. *Macromolecules* **1995**, *28*, 1066–1075.
- (13) Tanaka, F.; Edwards, S. F. *J. Nonnewtonian Fluid. Mech.* **1992**, *43*, 247.
- (14) Jones, M. *J. Colloid Interface Sci.* **1967**, *23*, 36–42.
- (15) Schwuger, M. J. *J. Colloid Interface Sci.* **1973**, *43*, 491–498.
- (16) Francois, J.; Dayantis, J.; Sabbadin, J. *Eur. Polym. J.* **1985**, *21*, 165–174.
- (17) Sakari, T.; Kushima, K.; Matsuda, K.; Suzuki, H. *Bull. Chem. Soc. Jpn.* **1980**, *53*, 1864–1866.
- (18) Chari, K.; Antalek, B.; Lin, M. Y.; Sinha, S. K. *J. Chem. Phys.* **1994**, *100*, 5294–5300.
- (19) Cabane, B. *J. Phys. Chem.* **1977**, *81*, 1639.
- (20) Cabane, B. *J. Phys. Fr.* **1982**, *43*, 1529–1542.
- (21) Moulik, S. P.; Haque, M. E.; Jana, P. K.; das, A. R. *J. Phys. Chem.* **1996**, *100*, 701–708.
- (22) Anthony, O.; Zana, R. *Langmuir* **1996**, *12*, 3590–3597.
- (23) Alami, E.; Almgren, M.; Brown, W.; Francois, J. *Macromolecules* **1996**, *29*, 2229–2243.
- (24) Almgren, M.; Hansson, P.; Mukhtar, E.; Stam, J. v. *Langmuir* **1992**, *8*, 2405.
- (25) Anthony, O.; Zana, R. *Langmuir* **1996**, *12*, 1967–1975.
- (26) Yekta, A.; Xu, B.; Duhamel, J.; Adiwidjaja, H.; Winnik, M. *Macromolecules* **1995**, *28*, 956–966.
- (27) Borisov, O. V.; Halperin, A. *Langmuir* **1995**, *11*, 2911–2919.
- (28) Fuller, G. G.; Leal, L. G. *J. Polym. Sci.: Polym. Phys. Ed.* **1981**, *19*, 531.
- (29) Stam, J. v.; Almgren, M.; Lindblad, C. *Prog. Colloid Polym. Sci.* **1991**, *84*, 13–20.
- (30) Stam, J. v.; Wittouck, N.; Almgren, M.; Schryver, F. C. D.; Miguel, M. d. G. *Can. J. Chem.* **1995**, *73*, 1765–1772.
- (31) Hulten, M. *Colloid Surf. A* **1994**, *82*, 263–277.
- (32) Persson, K.; Wang, G.; Olofsson, G. *J. Chem. Soc., Faraday Trans.* **1994**, 3555–3562.
- (33) Zhang, K.; B. Xu; Winnik, M. A.; Macdonald, P. M. *J. Phys. Chem.* **1996**, *100*, 9834–9841.
- (34) Annable, T.; Buscall, R.; Ettelaie, R.; Shepherd, P.; Whittlestone, D. *Langmuir* **1994**, *10*, 1060–1070.

MA9911593